World Scientific Research Journal (WSRJ) ISSN: 2472-3703
www.wsr-j.org

Pavement Crack Detection Method Based B-Cosfire Filters

Linyu Huang[1, a]

[1]Department of computer science and technology, Tongji University, Shanghai, China

[a]1290415778@qq.com

Abstract: Because of the multi-texture, multi-objective, weak signal of the target and the variability of the light intensity of the image, it is difficult to recognize the road crack target. This is a very important task, especially for detecting the situation surrounded by noise. A new detector based on cosfire filters model is proposed. By comparing other filtering methods, better segmentation results and stronger anti-noise ability are obtained on noisy data sets. At the same time, the feature extraction model and RGB channel can be used to construct a four-dimensional feature vector library for the classification of cracks types. It is an effective and anti-noise algorithm for pavement crack detection in the field of video and multimedia.
Keywords: Pavement crack detection, cosfire, anti-noise, non-linear filters.

---

1. INTRODUCTION

Pavement crack detection can be regarded as an application of linear and structural description. Linear structure is considered as one of the important features of classification because it provides geometric information of images. COSFIRE filter can describe the linear structure of the image, which makes COSFIRE filter play a significant role in a variety of computer vision applications, including vascular segmentation in medical images, road crack recognition, satellite cloud image of the river segmentation and so on.

The Hough transform is a classical method for extracting linear structures similar to cracks in an image. It maps the input image to the parameter space that detects the curve of interest. Other existing methods are based on feature transformation, mathematical morphology techniques and region growing, point and object processes, and machine learning methods.

Filters technique is based on multi-scale analysis of local derivative [1] or Gaussian kernel [2] to model line structure. Multi-scale information on directions, scales, and linewidths is also used for regional growth techniques [3]. A priori information about linear networks combined with mathematical morphology [4]. Then, the centerline of the thick line structure is the basic idea of the tracking method [5].

Point or object processes are used for line structure and target detection. In [6], a line network is obtained by object process modeling, where the object corresponds to an interactive line segment. The point process is generalized in [7] and [8], and the sampling process based on

Monte Carlo form and the random tag process based on Gibbs model are introduced respectively. The graph-based approach is also used to implement automatic tree reconstruction [10] and path classifiers using mixed integer programming. The structure information provided by the graph-based representation [9] is combined with the point processing based on the sampling nodes in the input image. Combine the point process with graph-based representation and classification to improve the accuracy of the segmentation. Since point processing and graph-based methods require high computational resources, the applicability of high resolution images is reduced.

In the pixel-based method, machine learning technology is used, in which pixel-by-pixel feature vectors are constructed and combined with the classifier system to distinguish linear and non-linear pixels. In the [11] and [12], the k-NN classifier is combined with the multi-scale Gauss lter and the ridge detector's response. In the [13], multi-scale Gabor wavelet modulus are used as training features of Bias classification. In [14], a set of bagged and reinforcement decision trees is proposed. In recent years, depth learning classifiers have been trained using line image blocks and used to extract blood vessels from retinal fundus images.

In this paper, we propose a pavement crack detector based on B-COSFIRE filter, which was originally proposed in [15], and applied them to the description of line structures in road crack images. The basic idea behind B-COSFIRE comes from the function of some neurons in the V1 region of the primary visual cortex, called simple cells, for detecting lines with different thicknesses. B-COSFIRE has trainable features and is easy to learn in the automatic modeling of a given pattern of interest.

The structure of the paper is as follows: in the second section, we give the proposed the structure of pavement crack detector. In the third section, we describe the data set and the experimental protocols we follow, compare our results with those reported in the literature, and discuss some aspects of the proposed method. Finally, we draw a conclusion in the fourth section.

2. METHOD

2.1 Physiological basis and mathematical model

Through long-term evolution and acquired growth, the visual nervous system of higher mammals can easily understand and recognize the surrounding environment, which is incomparable with computer vision system in all aspects. Therefore, it has become a hot issue in the field of computer vision to study the working mechanism of the visual system in higher mammals and how to make computers have such working mechanism of the visual nervous system.

The properties of the B-COSFIRE filter are stimulated by the function of some simple cells (also called neurons) in the primary visual cortex of the V1 region [16]. As described by Hubel and Wiesel [17] in their article, this simple cell (also called a neuron) is selective for a fine linear structure (linear, strip or contour).

(i)Receptive field of simple cells

Hubel and Wiesel studied the visual cortex of cats and found that the ability of choosing the direction of visual cortex V1 was due to the combination of LGN cell models. It should be more intense, and when deviated from this position, the response will weaken or disappear, so they conclude that the simple cell receptor field distribution is a narrow band-shaped central excitatory region. As shown in Fig1.

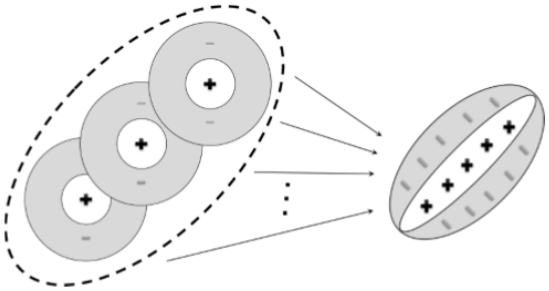

Fig 1. Computational model of a simple cell

(ii)Receptive field mathematical model

The classical receptive field is of great significance to human understanding of visual perception system. On this basis, researchers have proposed a number of mathematical computational models, such as Double Gauss Difference Model (DoG) model, Gabor model, to simulate the biological characteristics of the receptive field. The calculation model in this paper is based on the DoG model,as early as 1965, Rodieck et al. used the DoG model to simulate the concentric antagonistic spatial characteristics of retinal ganglion cells in cats [18-20].The following two formulas give one and two dimensional expressions of the DoG model.

$$\begin{aligned} DoG(x) &= G_1(x) - G_2(x) \\ &= \frac{1}{\sqrt{2\pi}\sigma_1}\exp(-\frac{x^2}{2\sigma_1^2}) - \frac{1}{\sqrt{2\pi}\sigma_2}\exp(-\frac{x^2}{2\sigma_2^2}) \end{aligned} \tag{1}$$

$$\begin{aligned} DoG(x,y) &= G_1(x,y) - G_2(x,y) \\ &= \frac{1}{2\pi\sigma_1^2}\exp(-\frac{x^2+y^2}{2\sigma_1^2}) - \frac{1}{2\pi\sigma_2^2}\exp(-\frac{x^2+y^2}{2\sigma_2^2}) \end{aligned} \tag{2}$$

Among them, σ_1 and σ_2 represent the spatial distribution of two Gauss distributions respectively.

Fig 2 shows the one-dimensional, two-dimensional and three-dimensional spatial distribution of the DoG model simulating the ON-type receptive field, where $\sigma_1 = 1$, $\sigma_2 = 0.5$. It can be seen that the spatial distribution of DoG model is similar to that of LGN cell receptor field sensitivity response model, which well simulates the spatial structure of concentric antagonistic cells. In addition, the DoG mathematical model has fewer parameters and clear physical meaning, so it is easier in engineering practice.

2.2 B-COSFIRE filters

Based on the physiological model and DoG mathematical model of complex cell receptor field, George et al. [15-16] proposed a B-COSFIRE filtering model. The filtering response was calculated by a set of geometric mean values of LGN cell computing models, which well simulated the working mechanism of complex cell receptor field. The sketch is shown in Figure 3.

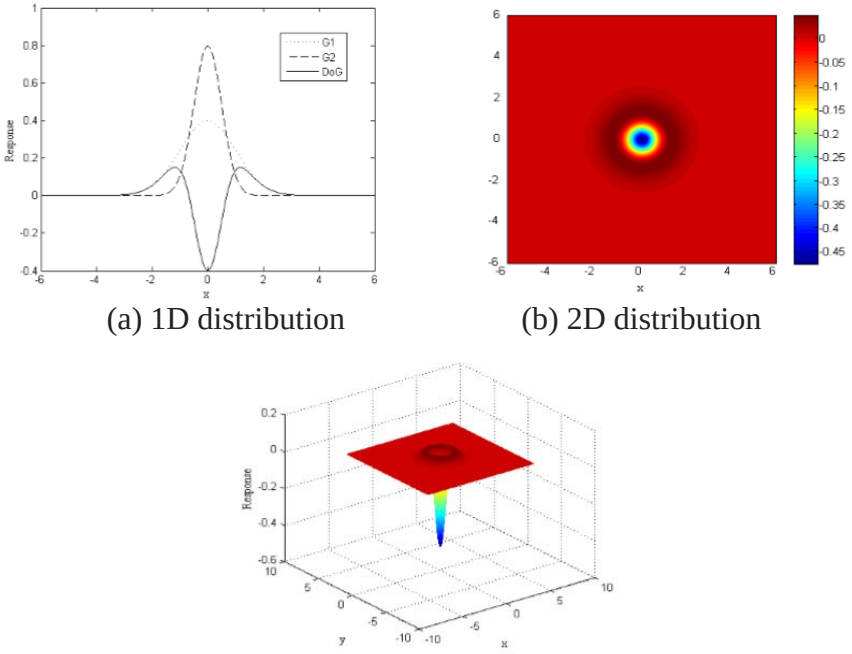

(a) 1D distribution (b) 2D distribution

(c) 3D distribution

Fig 2. Spatial distributions of the DoG model

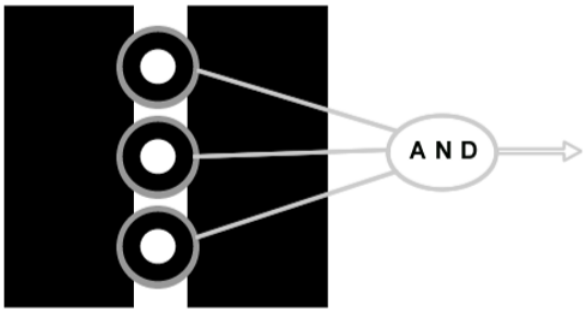

Fig 3. Structure of a B-COSFIRE filters. Gray disks represent the responses of a set of DoG filters, the output of the filter is multiplexed by such a group.

In this paper, two dimensional Gauss's function is used to simulate LGN cell receptive field model.

$$DoG_{\sigma}^{+}(x,y)=\frac{1}{2\pi\sigma^{2}}\exp(-\frac{x^{2}+y^{2}}{2\sigma^{2}})-\frac{1}{2\pi(0.5\sigma)^{2}}\exp(-\frac{x^{2}+y^{2}}{2(0.5\sigma)^{2}}) \quad (3)$$

As mentioned in electrophysiological studies [21], [22], we also set the standard deviation of the inner Gaussian kernel to 0.5We set the standard deviation of the inner Gaussian function to 0.5σ.

The B-COSFIRE filter, originally proposed in [15],acquires its input from a set of Gaussian difference (DoG) filters on a response to a specific position calculated on the input image I relative to the center of its support region.The notation $|\cdot|^{+}$ indicates a half-wave rectification operation, also known as Rectified Linear Unit (ReLU).

$$C_{\sigma}(x,y) \overset{def}{=} \left| I * DoG_{\sigma} \right|^{+} \tag{4}$$

In the proposed B-COSFIRE filter [15], three parameters $(\sigma_i, \rho_i, \phi_i)$ represented a point, where σ_i that provides input shows the standard deviation of the DoG filters, while ρ_i, ϕ_i represents the polar coordinates of the B-COSFIRE filter. Combination of three parameters of the B-COSFIRE filter is denoted by $S = \{(\sigma_i, \rho_i, \phi_i) \mid i = 1,...,n\}$.

In order to allow a certain intensity at a specific point, the blur operation of the DoG filter is shown in equation (5).

$$\sigma' = \sigma'_0 + \alpha\rho_i \tag{5}$$

Where σ'_0 and α are constants.

To coincide at the support center of the B-COSFIRE filter, the DoG blurred effect is moved a distance ρ_i in the opposite direction. For each tuple $(\sigma_i, \rho_i, \phi_i)$ in set S, the i_th blurred and shifted responses of the DoG filter are expressed as:

$$S_{\sigma_i,\rho_i,\phi_i}(x,y) = \max_{x,y}\{C_{\sigma_i}(x-\Delta x_i - x', y-\Delta y_i - y')G_{\sigma_i}(x',y')\} \tag{6}$$

Where $-3\sigma' \le x', y' \le 3\sigma'$.

The output of B-COSFIRE filters is defined as geometric mean of all the blurred and shifted DoG responses:

$$r_s(x,y) \overset{def}{=} \left| \left(\prod_{i=1}^{|S|} (S_{\sigma_i,\rho_i,\phi_i}(x,y))^{\omega_i} \right)^{1/\sum_{i=1}^{|s|}\omega_i} \right|_t \tag{7}$$

Where $\omega_i = \exp^{\frac{\rho_i^2}{2\sigma^2}}$ and $|.|_t$ represents thresholding response att($0 \le t \le 1$).When all DoG filter responses are greater than zero,the above equation is AND operation that is implemented by B-COSFIRE filter , Finally, AND operation between vessel map location output and B-COSFIRE filter result gives a composite binary image.

The direction selectivity of the B-COSFIRE filter depends on the direction of the prototype pattern used for configuration. In order to achieve tolerance for the rotation of the pattern of

interest, we process the parameter ϕ_i in the model S to obtain a new set $R_\psi(S)=\{(\sigma_i,\rho_i,\phi_i+\psi)\,|\,i=1,...,n\}$ which ψ represent orientation preference. We calculate the rotation tolerance response by taking the maximum response of each pixel in the responses of B-COSFIRE filters with different orientation preferences:

$$\hat{r}_s(x,y)\overset{def}{=}\max_{\psi\in\Psi}\left\{r_{R_\psi(S)}(x,y)\right\} \tag{8}$$

Where $\Psi=\left\{0,\frac{\pi}{n_r},\frac{2\pi}{n_r},...\frac{(n_r-1)\pi}{n_r}\right\}$ is a set of n_r preferred orientations. In this work, we apply the simple and public application of Matlab to achieve a B-COSFIRE filter model.

3. EXPERIMENTAL RESULTS

The common features of road crack images are gray features, texture features and geometric morphological features. After denoising and segmentation, the road crack images are binary images. The gray and texture information of the images have been lost, so it is not suitable to extract the gray and texture features. Geometric feature is one of the common features of road surface images. Different types of crack targets have different geometric shape characteristics. Crack geometry is a visual representation of the shape, is similar to the outline of such structural features, mainly through the distribution of pixels to reflect.

We use the road surface information collected by the camera installed in the lower part of the car as a data set and carry out experiments. The data set includes four different types of road surface cracks, namely, transverse cracks, longitudinal cracks, mesh cracks and block cracks.Binary images of different types of cracks are obtained. For evaluating performance, manual annotation of original images is also performed.

Because the actual road picture is more complex background conditions, such as the uneven light, the shadows of street lights, leaves and other debris shielding. All these have increased the difficulty in accurate detection of crack linear structures. Fig 4 shows the proposed method for detecting cracks in images with more prominent noise points and more complex background.It can be seen that the B-COSFIRE filter has better robustness to noise points.

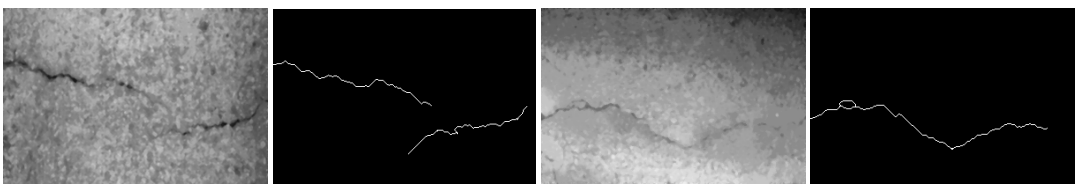

(a) (b) (c) (d)

Fig 4. (a) (c) Original image of more complex background (b)(d)Binary image of (a)(c)

In Table 1, we show the effectiveness of the proposed method on the data set from three indicators and run time, and compare the methods in other papers mentioned in this paper. B-COSFIRE obtained the highest MCC value. At the same time, it has much shorter processing

time than other methods, which is advantageous to the large-scale application of this method. In Table 2, we show the configuration parameters of the B-COSFIRE filter.

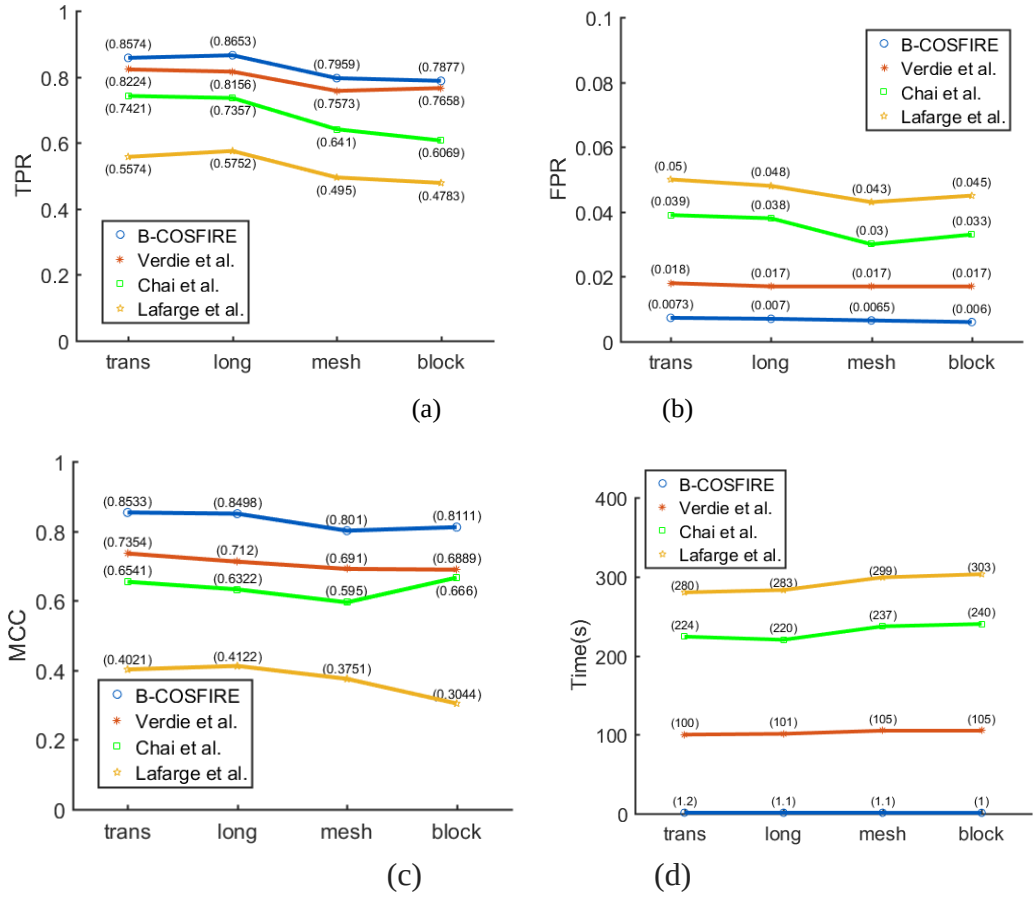

Fig 5. The TPR, FPR, MCC, and time values obtained by four different methods for data sets with different fracture types

B-COSFIRE has trainable characteristics, which can be regarded as a kind of learning. It can construct a recognizer to calculate salient features from the training samples. Compared with traditional pattern recognition methods, a series of features must be designed manually to describe the features, which requires a lot of prior knowledge and is not easy to optimize. B-COSFIRE is more similar than the popular method of deep learning. We can identify the key characteristics of the problem through self-learning of training samples.

Fig 5 shows the TPR, FPR, MCC, and time values obtained by four different methods for data sets with different fracture types. It can be seen that B-COSFIRE is superior to other method in these four indicators, and the detection effect of transverse and longitudinal cracks is superior to mesh and block cracks.

Table 1. Result comparison on data set

Method	TPR	FPR	MCC	Time
B-COSFIRE	0.8392	0.0066	**0.8410**	1.2s
Verdie et al.[8]	0.783	0.018	0.7128	102s
Chai et al.[9]	0.659	0.036	0.6271	230s
Lafarge et al.[7]	0.528	0.046	0.3821	295s

Table 2. Configuration parameters of the B-COSFIRE filter

Images	Parameters			
	σ	ρ	σ_0	α
Crack	1.4	$\{0, 2, ..., 8\}$	2	1.4

4. CONCLUSION

Pavement crack detection is of great significance for road disease diagnosis. For the uneven brightness of the shot, the noise points highlight the actual situation. The B-COSFIRE filtering method adopted in this paper has achieved good results on these problems. At the same time, it also has prominent advantages in running time, which is suitable for large-scale applications. It can be further optimized under the parallel processing environment. The structure used in the method also has the ability of self-adaptive learning, so it can be applied only to the detection of other linear structures.

REFERENCES

[1] A. F. Frangi, W. J. Niessen, K. L. Vincken, and M. A. Viergever, Multiscale vessel enhancement filtering. Berlin, Heidelberg: Springer Berlin Heidelberg, 1998, pp. 130–137.

[2] A. Hoover, V. Kouznetsova, and M. Goldbaum, “Locating blood vessels in retinal images by piecewise threshold probing of a matched filter response,” IEEE Transactions on medical imaging, vol. 19, no. 3, pp. 203–210, 2000.

[3] M. E. Martinez-Pe´rez, A. D. Hughes, S. A. Thom, A. A. Bharath, and K. H. Parker, “Segmentation of blood vessels from red-free and fiuorescein retinal images.” Medical Image Analysis, vol. 11, no. 1, pp. 47–61, 2007.

[4] A. M. Mendonca and A. Campilho, “Segmentation of retinal blood vessels by combining the detection of centerlines and morphological reconstruction,” IEEE Transactions on Medical Imaging, vol. 25, no. 9, pp. 1200–1213, 2006.

[5] O. Chutatape, Liu Zheng, and S. Krishnan, “Retinal blood vessel detection and tracking by matched Gaussian and Kalman filters,” in Proc. 20th Annu. Int. Conf. IEEE Eng. Med. Biol. Soc. (EMBS’98), H. Chang and Y. Zhang, Eds., vol. 17, no. 6, 1998, pp. 3144–9.

[6] C. Lacoste, X. Descombes, and J. Zerubia, “Point processes for unsupervised line network extraction in remote sensing,” IEEE Transactions on Pattern Analysis and Machine Intelligence, vol. 27, no. 10, pp. 1568– 1579, Oct 2005.

[7] F. Lafarge, G. G. farb, and X. Descombes, “Geometric feature extraction by a multimarked point process,” IEEE Transactions on Pattern Analysis and Machine Intelligence, vol. 32, no. 9, pp. 1597–1609, Sept 2010.

[8] Y. Verdie´ and F. Lafarge, Efficient Monte Carlo Sampler for Detecting Parametric Objects in Large Scenes. Berlin, Heidelberg: Springer Berlin Heidelberg, 2012, pp. 539–552.

[9] D. Chai, W. Forstner, and F. Lafarge, “Recovering Line-networks in Images by Junction-Point Processes,” in Computer Vision and Pattern Recognition (CVPR), Portland, United States, Jun. 2013.

[10] E. Tu¨retken, F. Benmansour, B. Andres, P. Gowacki, H. Pfister, and P. Fua, “Reconstructing curvilinear networks using path classifiers and integer programming,” IEEE Transactions on Pattern Analysis and Machine Intelligence, vol. 38, no. 12, pp. 2515–2530, Dec 2016.

[11] M. Niemeijer, J. Staal, B. van Ginneken, M. Loog, and M. Abramoff, “Comparative study of retinal vessel segmentation methods on a new publicly available database,” in Proc. of the SPIE - The International Society for Optical Engineering, 2004, pp. 648–56, Medical Imaging 2004. Image Processing, 16-19 Feb. 2004, San Diego, CA, USA.

[12] J. Staal, M. Abramoff, M. Niemeijer, M. Viergever, and B. van Ginneken, “Ridge-based vessel segmentation in color images of the retina,” IEEE Transactions on medical imaging, vol. 23, no. 4, pp. 501–509, 2004.

[13] J. V. B. Soares, J. J. G. Leandro, R. M. Cesar, Jr., H. F. Jelinek, and M. J. Cree, “Retinal vessel segmentation using the 2-D Gabor wavelet and supervised classification,” IEEE Transactions on medical imaging, vol. 25, no. 9, pp. 1214–1222, 2006.

[14] M. Fraz, P. Remagnino, A. Hoppe, B. Uyyanonvara, A. Rudnicka, C. Owen, and S. Barman, “An ensemble classification-based approach applied to retinal blood vessel segmentation,” IEEE Transactions on Biomedical Engineering, vol. 59, no. 9, pp. 2538–2548, 2012.

[15] G. Azzopardi, N. Strisciuglio, M. Vento, and N. Petkov, “Trainable cosfire filters for vessel delineation with application to retinal images,” Medical Image Analysis, vol. 19, no. 1, pp. 46 – 57, 2015.

[16] G. Azzopardi and N. Petkov, “A CORF computational model of a simple cell that relies on LGN input outperforms the Gabor function model,” Biological Cybernetics, vol. 106, no. 3, pp. 177–189, 2012.

[17] D. Hubel and T. Wiesel, “Receptive fields, binocular interaction and functional architecture in the cat’s visual cortex,” Journal of PhysiologyLondon, vol. 160, no. 1, pp. 106–&, 1962.

[18] Xu X., Bonds A., Casagrande V. Modeling receptive-field structure of koniocellular, magnocellular, and parvocellular LGN cells in the owl monkey (Aotus trivigatus)[J]. Visual Neurosci, 2002, 19: 703–711.

[19] Rodieck R. W., Stone J. Analysis of receptive fields of cat retinal ganglion cells [J]. Journal of Neurophysiology, 1965, 28(5): 833-849.

[20] Croner L. J., Kaplan E. Receptive-fields of P-ganglion and M-ganglion cells across the primate retina [J]. Vis Res, 1995, 35(1): 7–24.

[21] G. Irvine, V. Casagrande, and T. Norton, “Center surround relationships of magnocellular, parvocellular, and koniocellular relay cells in primate lateral geniculate-nucleus,” Visual Neuroscience, vol. 10, no. 2, pp. 363– 373, 1993.

[22] X. Xu, A. Bonds, and V. Casagrande, “Modeling receptive-field structure of koniocellular, magnocellular, and parvocellular LGN cells in the owl monkey (Aotus trivigatus),” Visual Neuroscience, vol. 19, no. 6, pp. 703–711, 2002.